Asian Journal of Chemistry; Vol. 24, No. 9 (2012), 4225-4231

ASIAN JOURNAL OF CHEMISTRY

www.asianjournalofchemistry.co.in

A Porous SiC Mat for a Gas Radiation Application by Melt-Blown of the Polycarbosilane†

DONG-GEUN SHIN[1], KWANG-YOUN CHO[2] and DOH-HYUNG RIU[3,*]

[1]SiC lab, LG Innotech, 1271 Sa 3 dong Sangrokgu Ansansi Gyoungi, 426-910, South Korea
[2]Nanotechnology Conversions Team, Korea Institute of Ceramic Engineering and Technology, 233-5 Gasan-dong, Guemcheon-gu, Seoul, 153-801, South Korea
[3]Department of Materials Science, Seoul Natinal University of Science and Technology, 232 Gongnungro Nowongu Seoul, 139-800, South Korea

*Corresponding author: Fax: +82 2 26446277; Tel: +82 2 26446276; E-mail: dhriu15@seoultech.ac.kr

AJC-11358

A porous SiC mat was fabricated by melt blown, curing and pyrolysis of a rheology controlled polycarbosilane. Polycarbosilane has undergone the two step polymerization to get the proper rheology for melt blown. The SiC fibers derived from KNAl-0002 were randomly distributed and stacked layer by layer. The melt blown mat was pressed down at low pressure of 0.2-0.4 kg/cm^2 during the curing process to build physical connections among the fibers and finally formed chemical bonds at the contact points after pyrolysis. The neck was also formed among the fibers in the crossing or parallel patterns. In the bending test, the SiC mat was restored to the initial shape after the removal of the compressive load under 50 g. The oxidation layer constantly formed on the fiber periphery without any cracks or pores at the boundaries was considered to be an excellent thermal protective layer. Infra-red radiation effect was also investigated in the fuel gas firing using a commercial gas burner.

Key Words: Silicon carbide mat, Infra-red radiation, Rheology, Melt blown, Polycarbosilane.

INTRODUCTION

A gas-fired radiant burner in which fuel gas is combusted in the form of free flame at the surface of radiant plate has been developed for cook-stove or pulp dryer in the last decade[3]. In this system, combustion usually happens inside of a radiant plate and the combustion energy is transferred to the plate making an infra-red radiation. The radiation properties of a burner is affected by the flame stability and flame structure include CO and NO_x emissions during combustion and these are controlled by the optical thickness, scattering properties and thermal conductivity of the radiant plate[1,5,6]. Radiant plate such as honeycomb, foam and fibrous one[2,4,6] have been developed to make efficient radiant systems for uniform heating of object surface with complete and clean combustion. High surface area of the radiant plate makes a complete combustion leading the strong radiation by the formation energy during the combustion[5].

Together with the high surface area of the radiation surface, the colour of the heater plate is also of main concern in order to obtain black body radiation efficiency. Therefore, SiC/SiC porous composites have been developed as an efficient radiation burner plates for pulp dry system. For the fabrication of the porous composites for radiant plate of a gas stove, long-continuous fiber chopped into a proper length, arrayed in a regular manner and subsequently coated with carbon and silicon carbide through CVD process[7]. The CVD process was essential for the composites to maintain the fiber to fiber contact that keeps the porous SiC fiber composite integrity during usage. However, the process is very expensive and complicate process and difficult the commercial application.

In this study, we have investigated an efficient way of forming porous SiC fiber composites using a simple *in situ* process. That is using a melt blown process and subsequent bonding of the melt blown fibers together by the curing and pyrolysis under the minimum amount of applied pressure. By this process, we can obtain the ceramic mat having high surface area and a point contact at the inter-section among the fibers. This type of minimum point to point contact of fibers can effectively protect the heat transfer from the upper surface to bottom of the plate and also make it strong enough for handling during the operation[6-9].

We have previously reported the fabrication of non-woven SiC mat by melt blown[10] and electrospinning process[11] derived from preceramic polymer[12], polycarbosilanes (PCS)[13]

†Presented to The 5th Korea-China International Conference on Multi-Functional Materials and Application.

catalytically converted from polydimethylsilane at a moderate condition[14,15]. The melt blown is a very simple and effective process for producing SiC mat having micron size diameters in which the rheological property of polycarbosilane is very important since it has an influence on the spinnability and the following process. In this study, polycarbosilane was synthesized and adjusted its rheology. A porous SiC mat was fabricated by melt blown of polycarbosilane and its structure, thermal and mechanical properties were investigated and related to the rheology. The radiation effect was also investigated for the application in a gas fired radiation burner.

EXPERIMENTAL

Polycarbosilane was synthesized from the Kumada rearrangement of polydimethylsilane (PDMS) under normal pressure in the presence of wired or powdery solid acid catalyst[16-18]. The mixture of 1 kg of polydimethylsilane and 10 g of catalyst was loaded into the reaction vessel. After purging the sample with argon gas, the reaction vessel was heated to 350 and 400 ºC in two-step for the conversion of polydimethylsilane into polycarbosilane and subsequent polymerization. It was further polymerized at 400 ºC for 5-10 h without catalyst after distilled out of the low molecular portion to get the proper rheology for melt blown process. The rheology of polycarbosilane was characterized by measurement of melting point [spindle (18) type apparatus; Electrotherm], molecular weight distribution (gel-permeation chromatography (GPC); Waters 2414 refractive index detector, 515 HPLC pump) and melt viscosity (viscometer; DV-II+, Brookfield). Table-1 shows the summaries of the properties of polycarbosilane.

TABLE-1
RHEOLOGICAL PROPERTIES OF POLYCARBOSILANE

Polycarbosilane	GPC			Melting point
	HM_w	MM_w	PDI	T_m
KNAl-0001	3290	700	2.38	180-240
KNAl-0002	3320	710	2.69	210-270

The melt blown system is simply comprised three parts as shown in Fig. 1: a spinning part including the melting vessel and spinning head, a collecting part and hot-air supplier including the heat exchanger and high pressure air compressor. Polycarbosilane having proper rheology was grinded into powder or granule and fed into melting vessel before controlling the inert atmosphere. The spinning part and the heat exchanger were slowly heated to spinning temperature with low pressure air blowing. When the system was reached to spinning condition, the polycarbosilane melt was spun out of the nozzle through the gear pump controlling the quantity of the polycarbosilane melt and the hot-air hits the spun melt into winding receiver (metal mesh). The fiber size and met porosity were controlled by the feed rate and the blowing air pressure. Samples with a diameter of 20 mm were taken from the melt blown mats and were subjected to the thermal curing at 200 ºC for 1 h in a muffle furnace with uniform pressing at low pressure (0.2-0.4 kg/m^2) for inducing the physical contacts among fibers and then sintered at a temperature of 1200 ºC for 1 h under a

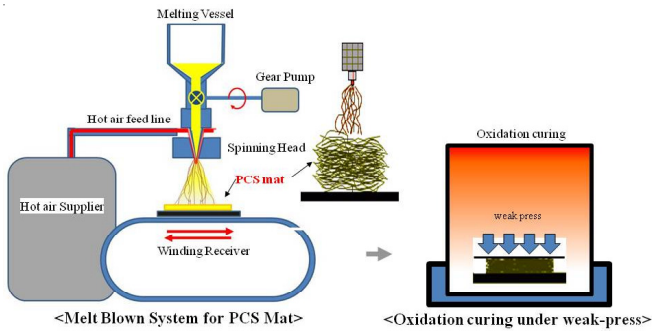

Fig. 1. Experimental setup of melt blown and thermal oxidation process

flowing argon atmosphere in a graphite furnace. The 3-point bending test was carried out using universal testing machine (UTM; Instron 4204 model) on the sample whose size is 5 mm × 40 mm. Gauge length was chosen to 30 mm and the cross-head speed was 1 mm/min. The microstructure and morphology of the melt blown mat and that of a single fiber were observed using a field-emission scanning electron microscope (FE-SEM; JSM-6700F, JEOL, Japan) operating at 15 kV. A thermo-gravimetry analyzer (TGA; TGA/SDTA 851, Mettler Toledo, USA) was used to analyze the pyrolysis behaviour of the SiC mat. A sample (10 mg) of the cured mat was roughly chopped and loaded into an alumina crucible and slowly heated (5 ºC/min) to 1200 ºC in an induction furnace under an argon atmosphere. During the heating process, the weight change was continuously monitored. The structure of the mat was characterized by X-ray diffraction (XRD; FR-150, Enraf-Nonius Co, Netherlands). The gas radiation heating test was performed by the measurement of the temperature profile of the SiC mat covered with the glass plate and the exhaust gas was measured using gas chromatography (GC; Hewlett-Packard, HP 5890 II). The tip of an acquisition probe (D = 2 mm and L = 450 mm) was quenched by cooling water for preventing the oxidation of the exhaust gas.

RESULTS AND DISCUSSION

The relation of the viscosity with the heating temperature was investigated to determine the proper spinning condition and presented in Fig. 2. The viscosities of the samples exponentially decreased as temperature increases following the Andrade equation[19,20]. Fig. 3(a) shows a softening of the viscosity around 140 ºC and its saturation up to 200 ºC whereas (b) shows a higher softening temperature 220 ºC. These viscous behaviours can be affected by the molecular shape, structure and the molecular weight distribution of PCS. Fig. 3 shows the GPC curves for the different conditions of (a) KNAl-0001 and (b) KNAl-0002. Two peaks are noticeable: middle molecular weight distribution (MM_w) and high molecular weight distribution (HM_w). Middle molecular weight distribution was mainly detected at the elution time around 24 min and the peak of high molecular weight distribution was observed at the shoulder around 22 min. The sharp peak at 0.5 h is from the toluene used as a solvent. High molecular weight distribution was shifted to left (higher molecular weight direction) and its relative intensity was also increased with the polymerizing time as shown in the Fig. 3(b) and (c). High molecular weight distribution in the polycarbosilane with molecular shape of

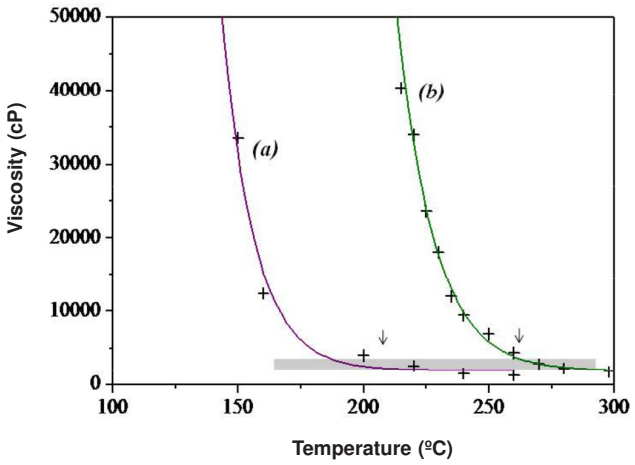

Fig. 2. Viscosity changes of (a) as-synthesized PCS, (b) KNAl-0001 and (c) KNAl-0002 with elevated temperature

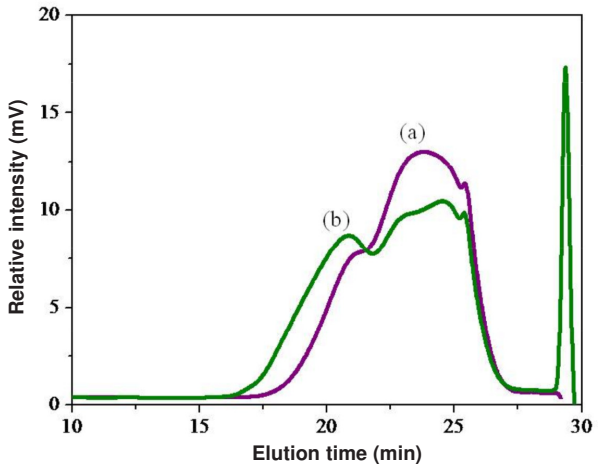

Fig. 3. GPC curves for (a) KNAl-0001 and (b) KNAl-0002

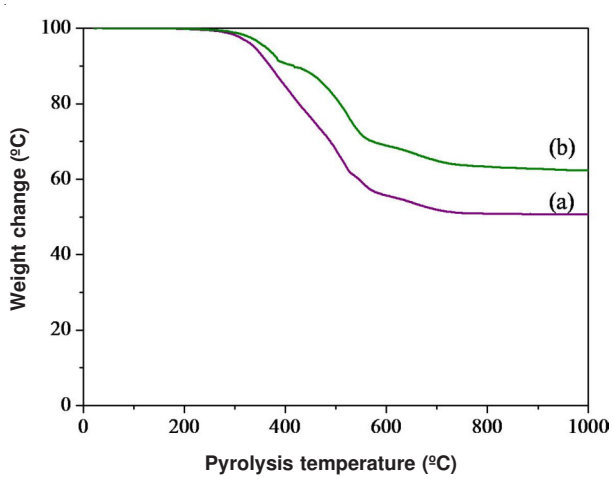

Fig. 4. TGA analysis of (a) KNAl-0001 and (b) KNAl-0002

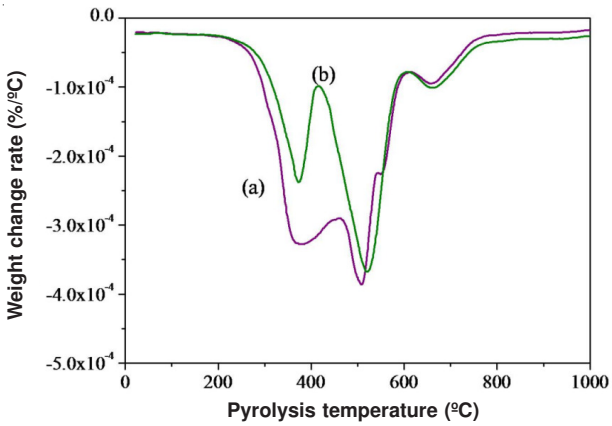

Fig. 5. DTG curves of (a) KNAl-0001 and (b) KNAl-0002

rather plate-like than linear shows high viscosity and low spinnability[21-23]. On the other hand, middle molecular weight distribution shows relatively linear molecular shape shows better spinnability[21,23]. Thus, the difference of the relative ratio of high molecular weight distribution and middle molecular weight distribution can cause the viscosity changes. Ideskai *et al.*[20] have reported the proper viscosity ranges having a good spinnability for melt-spinning of polycarbosilane are 5000-10000 cP[20]. However, thermal curing condition limits the spinnable temperature to be over 200 ºC. It was found that the optimum temperature for melt-blown of KNAl-0001 and KNAl-0002 was 200 and 260 ºC where the melt viscosity was 3000-5000 cP. They were melt blown at each spinnable condition and polycarbosilane fibers were randomly distributed on the receiver stacked layer by layer.

Fig. 4 shows the TGA analysis and Fig. 5 shows the DTG analysis of (a) KNAl-0001 and (b) KNAl-0002. The weight was reduced at the temperature between 200 and 700 ºC and the reduction was dominant below 500 ºC. The final ceramic residue was remained only 51 % in KNAl-0001 (a) whereas 62 % in KNAl-0002 (b) and the reducing steps were slightly different. The reduction rate in the DTG curves (Fig. 5) shows that the three major reductions in the samples. In case of the pyrolysis of polycarbosilane, methylsilane or some evaporated portions are removed at the first step and C_2H_6, CH_4, H_2 and O_2 gases are subsequently decomposed out at the second and third step[15,24,25]. At this time, the weight reduction curve (b) was slightly shifted to higher temperature than the other curve (a). It is because (b) has higher contents of high molecular weight distribution than KNAl-0001 and will affect the characteristics of SiC mat after curing and pyrolysis.

The weight reduction by pyrolytic decomposition is also related to decrease in the size of the prepared mat. Fig. 6 shows the photographs of (a) polycarbosilane mat cured at 200 ºC for 1 h and (b) SiC mat pyrolyzed (a) at 1200 ºC for 1 h. The polycarbosilane mat has transparent yellow colour and was cut into circular shape with diameter of 200 mm before curing. It pressed down into 2.0 kg/cm^2 during the curing process and pyrolysis at 1200 ºC under inert atmosphere spontaneously. Size of the mat wasn't changed after curing, but it reduced to 150 mm after pyrolysis.

Fig. 7 shows FESEM images of the SiC mat: surface images of (a) KNAl-0001 and (b) KNAl-0002 and (c) is a cross-sectional image of KNAl-0002. In Fig. 7(a), all the fibers in the mat were considerably melted and tangled each other by forming round shapes of inter-fiber pores of 20-200 μm. On the other hand, Fig. 7(b) shows the circular cross section and the straight arrangement of the fibers wider than the diameter of 10 μm are not changed. In the figure, smaller fibers were shown randomly distributed among the wider fibers. Every layer was uniformly

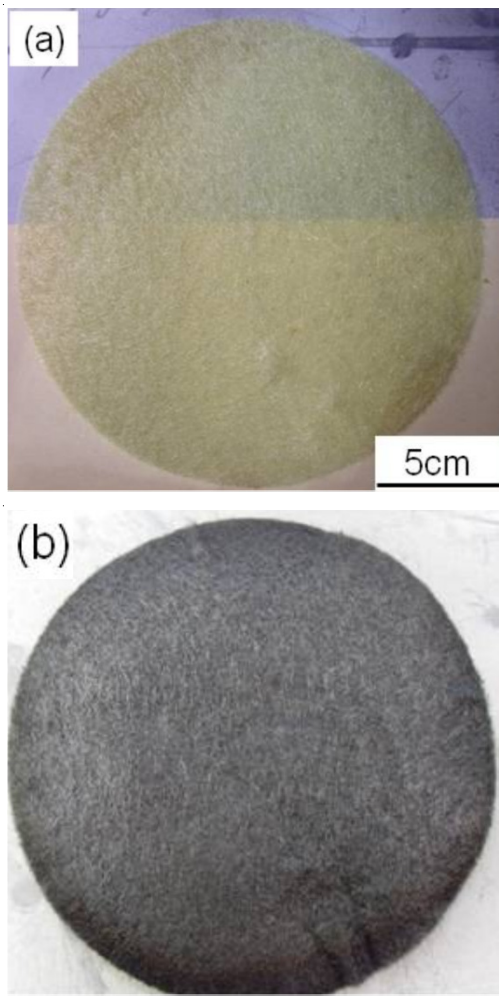

Fig. 6. Photograph images of (a) polycarbosilane mat melt blown and cured of KNAl-0002 at 220 ºC and (b) SiC mat pyrolyzed (a) at 1200 ºC

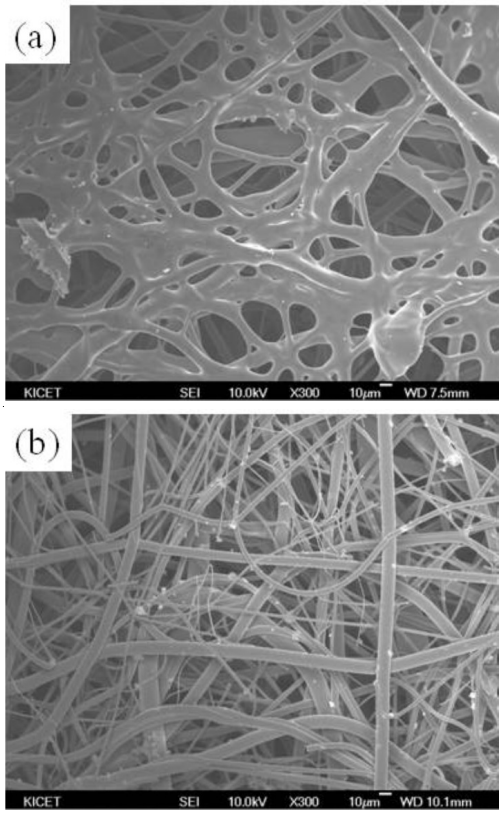

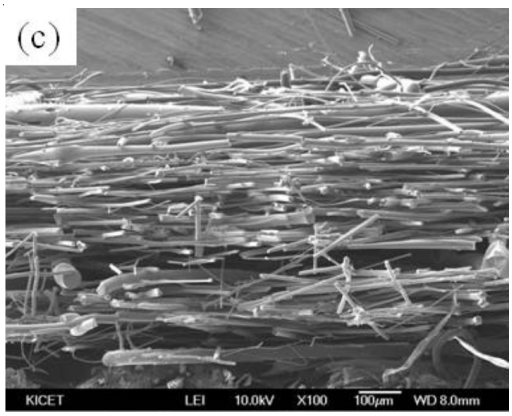

Fig. 7. FESEM images of SiC mat pyrolyzed at 1200 ºC for 1 h; surface of (a) KNAl-0001 and (b) KNAl-0002 and (c) cross-sectional image of KNAl-0002

stacked through the transverse directions like a fagot and each layer was also connected through the point contacts. High-magnificent view of SiC mats derived from KNAl-0002 were shown in Fig. 8 that presents the detail feature of inter-fiber connection at the point contacts. Fibers were randomly arranged during the melt blown process and pressed down to form physical contacts at low pressure of 0.2-0.4 kg/cm^2 and finally formed chemical bonds, so-called "the neck" at the contact points during the pyrolysis process. They were formed in the crossing or parallel patterns and distributed uniformly all over the SiC mat. The detail microstructures can provide quite different mechanical behaviours. KNAl-0001 was pretty hard and scarcely bended while KNAl-0002 was flexible under sufficient load. The result of 3-point bending test in the Fig. 9 shows the effect of the "point contact structure" on the relative strength and the flexibility for each mat. Fig. 9(a) shows the load-distance curve of KNAl-0001 showing the initial stiff increase of the load at the beginning and fractured at 128 g. On the other hand, the curve of KNAl-0002 in Fig. 9(b) slowly increase to about 50 g and sustain the constant load until the compressive displacement up to 5 mm and can restore to its original shape after the removal of the load.

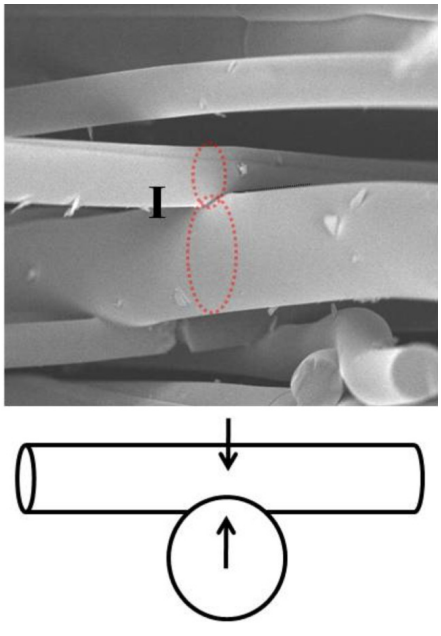

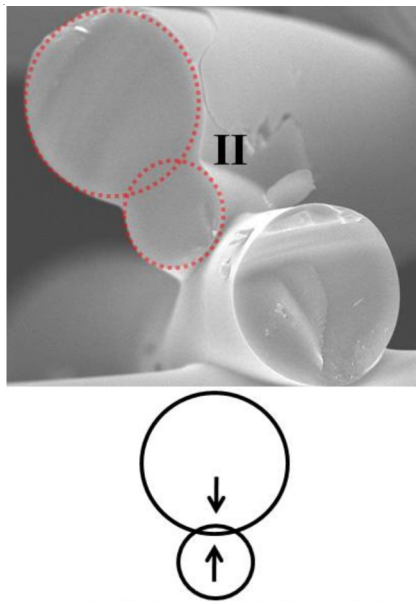

Fig. 8. High magnificent FESEM images of SiC mat pyrolyzed the PCS mat derived from KNAl-0002 at 1200 ℃ for 1 h; I and II show the inter-fiber contacts (necking)

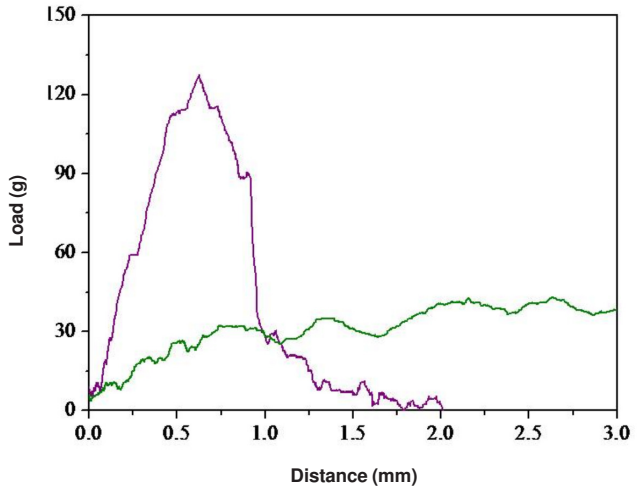

Fig. 9. Load-distance curves for 3-point bending test of SiC mat derived from (a) KNAl-0001 and (b) KNAl-0002

In order to examine the SiC mat after pyrolysis at 1200 ℃ for 1 h under argon atmosphere, it was crushed into a powder and analyzed with XRD. Fig. 10 shows the XRD pattern of SiC mat derived from KNAl-0002 pyrolyzed at 1200 ℃ after cured at 200 ℃ for 1 h under mild compression. The diffraction peaks at around 35.7, 60 and 71.8º corresponded to cubic β-SiC which were attributed to the (111), (220) and (311) planes. All the peaks were quite broad because the nanocrystalline β-SiC are dispersed among amorphous Si-O-C matrix which indicated that the SiC fiber was in the early stage of crystallization at this heat treatment temperature[16,18,26]. The second phase such as graphite or silica couldn't be found in the XRD pattern.

Silicon carbide mat was examined for the behaviour maintained in the atmospheric muffle furnace for 1, 12, 24 and 48 h at 1000 ℃. There was no significant difference in weight change during the oxidation until 48 h. The facture surface of oxidized fiber in the SiC mat was observed using

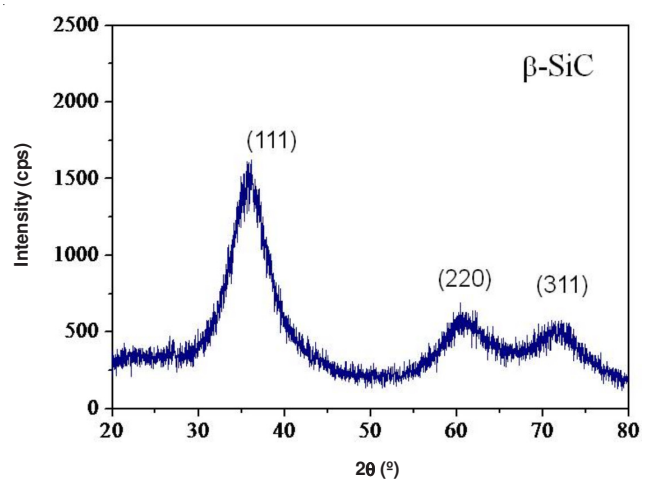

Fig. 10. X-Ray diffraction pattern of SiC mat pyrolyzed the PCS mat derived from KNAl-0002 at 1200 ℃ for 1 h

FESEM and showed in the Fig. 11. When the SiC mat was exposed to the oxidation atmosphere at 1000 ℃ for 48 h, the fibers were uniformly coated with a smooth oxide layer of about 380 nm and the thickness was constant along the fiber periphery without any cracks or bubbles at the boundaries. The oxide layers were also observed at the neck and there wasn't any degradation even at the sharp node. It is expected that uniform layer will slow down the oxidation rate and act as an excellent oxidation protective layers during the operation[26,27].

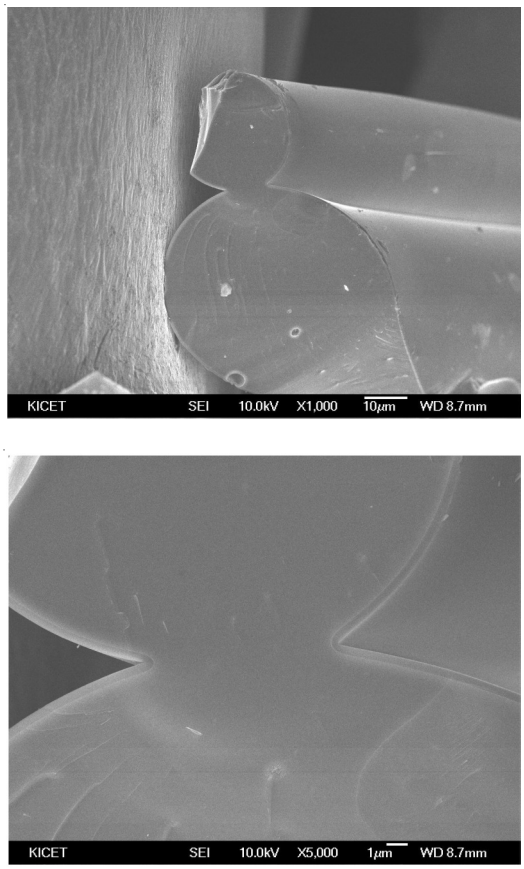

Fig. 11. High magnificent FESEM images of SiC mat oxidized at 1000 ℃ for 48 h

The infrared radiation effect of the SiC mat was tested using commercial gas burner. Silicon carbide mat was equipped on top of the combustor covered with the flame protecting glass and operated at the adjusted gas mixing ratio (butane:air). Infrared was radiated all over the mat during the operation. The temperature was also measured by the colour profile as shown in the Fig. 12 and the temperature on the glass reached to 530 ºC. However, it was still lower than conventional radiant plate. It is because SiC mat wasn't sufficiently heated up to high temperature which was required to burn a fuel gas completely. The results of GC analysis support this incomplete combustion behaviour in the mat. Fig. 13 shows the combustion gas evolution with cross-sectional distance of the SiC mat. Carbon monoxide gas was detected to 1600 ppm where oxygen was reached to zero percent. In general, carbon monoxide gas is not evolved at the stable radiation flame through the optimum oxygen supply condition[3]. However, insufficient oxygen supply into the SiC mat makes carbon monoxide gas in the luminous (flame orange colour) region. It makes the low surface temperature of the radiation mat and can be considered that the pore size in the mat was scarcely large enough to flow a mixed gas easily[15].

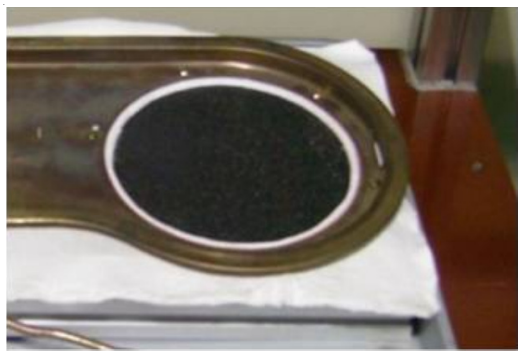

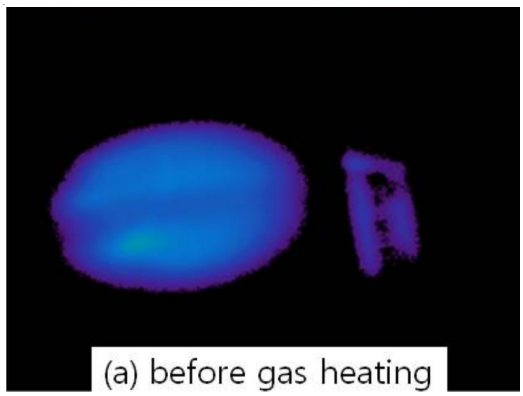

Fig. 12. Temperature profile of SiC mat covered with the glass plate (a) before and (b) after gas radiation heating test

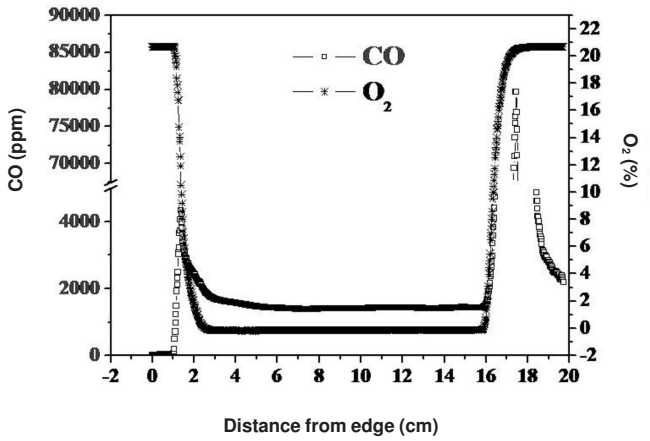

Fig. 13. GC analysis of SiC mat during a fuel gas combustion

Conclusion

A porous SiC mat was successfully fabricated by melt blowing and pyrolysis of a rheology controlled polycarbosilane. The SiC mat derived from KNAl-0002 had a bimodal fiber distribution from 1-3 μm to 7-15 μm. Each layer was stacked well through the transverse directions and chemically bonded at the contact points. This bond structure was affected by the rheology of polycarbosilane and made a SiC mat very flexible and strong enough for handling during the operation. Furthermore, oxidation layer was formed uniformly on the fiber periphery without any cracks or pores at the boundaries and it will act as an excellent thermal protective layer. Finally, IR radiation was observed all over the mat surface. However surface temperature was lower than conventional one and CO gas was evolved due to the incomplete combustion during the burning process.

ACKNOWLEDGEMENTS

This research was partly supported by the MKE (Ministry of Knowledge Economy), Korea and partly supported by Seoul National University of Science and Technology, Korea.

REFERENCES

1. T.-W. Tong and W.J. Li, *Quant. Spectrosc. Radiat. Transfer*, **53**, 235 (1995).
2. M.-A. Mujeebu, M.-Z. Abdullah and A.-M. Abdullah, *Appl. Energy*, **86**, 1365 (2009).

3. Y.-S. Kim, S.-W. Cho, G.-B. Kim, Y.-J. Chang and C.-H. Jeon, *Trans. KSME B*, **31**, 539 (2007).
4. S.-B. Sathe, R.-E. Peck and T.-W. Tong, *Int. J. Heat Mass Transf.*, **33**, 1331 (1990).
5. M.-R. Kulkarni and R.-E. Peck, Proceedings of Joint Meeting of Central and Western States Section and Mexican National Section of the Combustion Institute and American Flame Research Committee, p. 26 (1995).
6. S. Hanzawa and T. Komiyama, US Patent 5,542,194 (1996).
7. R.-U. Hasse and M. Kahlke, US Patent 5,800,157 (1998).
8. M. Kahlke, C. Koster and R. Hasse, US Patent 6,076,517 (2000).
9. Y. Yamada, T. Sobue and M. Oyaizu, 22nd WGC Technical Forum, Poster Presentation (TF 6-C), Jun 1-5 (2003).
10. D.-H. Riu, D.-G. Shin, E.-B. Kong, Y. Kim, H.-J. Hong, K.-Y. Cho and S.-H. Huh, *Ceramist*, **4**, 54 (2007).
10. T. Ishikawa, K. Bansaku, N. Watanabe, Y. Nomura, M. Shibuya and T. Hirokawa, *Comp. Sci. Technol*., **58**, 51 (1998).
12. H. Araki, W. Yang, H. Suzuki, Q. Hu, C. Busabok and T. Noda, *J. Nucl. Mater*., **32**, 567 (2004).
13. N. Igawa, T. Taguchi, T. Nozawa, L.-L. Snead, T. Hinoki, J.-C. McLaughlin, Y. Katoh, S. Jitsukawa and A.J. Kohyama, *Phys. Chem. Solids*, **66**, 551 (2005).
14. D.-G. Shin, D.-H. Riu, Y. Kim, Y.-K. Jeong, H.-S. Park and H.-E. Kim, *Key Eng. Mater*., **91**, 287 (2005).
15. D.-G. Shin, D.-H. Riu and H.-E. Kim, *J. Ceram. Process. Res*., **9**, 209 (2008).
16. S.-H. Huh, D.-G. Shin, D.-H. Riu, E.-J. Jin, E.-B. Kong, K.-Y. Cho, C.-Y. Kim and H.-E. Kim, *Catal. Commun*., **10**, 208 (2008).
17. D.-H. Riu, S.-J. Kim, D.-G. Shin, H.-R. Kim and Y.-H. Kim, *J. Ceram. Soc. (Japan)*, **112**, S432 (2004).
18. Y.-H. Kim, S.-J. Jung, H.-R. Kim, H.-D. Kim, D.-G. Shin and D.-H. Riu, *Adv. Technol. Mater. Mater. Proces*, **6**, 192 (2004).
19. E.N. Andrade, *Nature*, **128**, 835 (1931).
20. A. Idesaki, M. Narisawa, K. Okamura, M. Sugimoto, S. Tanaka, Y. Morita and T. Seguchi, *J. Mater. Sci*., **36**, 5565 (2001).
21. Y. Hasegawa and K.J. Okamura, *Mater. Sci*., **21**, 321 (1986).
22. X. Cheng, Z. Xie, J. Xiao and Y. Song, *J. Inorg. Org. Polym. Mater*., **15**, 253 (2005).
23. S. Yajima, Y. Hasegawa, K. Okamura and T. Matsuzawa, *Nature*, **273**, 525 (1978).
24. G. Chollon, M. Czerniak, R. Pailler, X. Bourrat, R. Naslain, J.-P. Pillot and R.-J. Cannet, *Mater. Sci*., **32**, 893 (1997).
25. E. Bouillon, F. Langlais, R. Pailler, R. Naslain, F. Curege, P.-V. Huong, J.-C. Sarthou, A. Delpuech, C. Laffon, P. Lagarde, M. Monthioux and A. Oberlin, *J. Mater. Sci. Lett*., **2**, 1333 (1991).
26. M. Takeda, A. Urano, J. Sakamoto and Y. Imai, *J. Am. Ceram Soc*., **83**, 1171 (2000).
27. T. Shimoo, Y. Morisada and K. Okamura, *J. Mater. Sci*., **37**, 4361 (2002).